

Confinement within the use of Minkowski integral representation

V. Šauli¹

¹*Department of Theoretical Physics, NPI Rez near Prague, Czech Academy of Sciences*

We determine the gluonic spectral function $SU(3)$ Yang-Mills theory as well as we found fermionic spectral functions in the strong quenched QED where we found new solutions. Our novel technique provides solutions with the usual branch cut for propagators while not showing any pole structure at the first Riemann sheet (identical with entire complex plane) of complex square of momentum. Implications and further utilizations are briefly adressed for QCD and Standard model calculations.

PACS numbers:

I. INTRODUCTION

Confinement is one of essential features of QCD, and whilst it is intuitively well understood as impossibility to observe the excitations of quark and gluon fields as a particle in isolation, a commonly accepted mathematically rigorous explanation of this phenomena is still missing.

Apart of QCD, QED_{2+1} as known from many studies [1–8] is a simple theory showing confinement. Notably, it serves as an effective theory in condense matter physics and physics of graphene [9] for many years. Here we argue, that for the coupling is strong enough, confinement exists in quenched QED_{3+1} as well. The value of the coupling where the fermion stop from being free particles coincides with the critical coupling of chiral symmetry breaking in theory with hard cutoff.

In presented paper we revise the numerical method based on utilization of integral representation for QED and $SU(3)$ Yang-Mills theory, more complicated issue of confinement of quarks in entire QCD theory is briefly mentioned, but not solved here.

In principle, theoretical search for a confined modes in QFT could be equivalent for proving of the absence of particle modes in the time ordered product of associated field: the quark and the gluon propagators, in QCD for instance. For this purpose we follow the integral representation methods [10–24] developed for purpose of solution of Schwinger-Dyson equations (SDEs). These methods offer the solution in the entire Minkowski space and the presence or absence of particle modes can be very obvious: one can or one does not see the on mass shell pole in the propagator (unphysical poles that do not appears in S-matrix are allowed, they can emerge in special choices of gauge and renormalization schemes and we do not discussed them here. In models considered here, the only example is the massless pole in longitudinal part of the gauge propagator). Owing to other gauges a different confinement pictures have emerged in history. The Gribov-Zwanziger picture of confinement [25],[26] is established in Coulomb gauge [27], while not confirmed in the class of linear gauges (e.g. in Landau gauge), where the lattice simulation of ghost propagator does not show enhancement- the required condition for the Gribov-Zwanziger scenario. Other scenario of confinement- the vortex condensation [28–33] with associated condensation of magnetic monopoles are detected on lattices in special gauges [34],[35],[36], e.g. in maximal Abelian gauge [37]. Obviously, different manifestation and realizations of confinement exist in various gauges, while they do not show up in other gauges.

To get the resulting form of propagators in the entire Minkowski space, there are several existing methods in hand. In principle, one can apply Schlessinger method of analytical continuation on the already known solution of SDEs obtained by conventional method in the Euclidean space [38, 39] (for the topic of SDEs see [40, 41]). In the study [38] the method confirms well known fact that the analytical property are affected by the truncation of SDEs, e.g. by the analytical properties of kernels which approximate unknown Green's functions that have been truncated out of the SDEs system. Actually, there exist well known models, where number of complex conjugated poles are supposed to be a part of the spectrum of calculated propagator. Using other methods, the analytical continuation of lattice propagators has been questioned in papers [42, 43], showing the answer is still very ambiguous. Furthermore, complex poles necessarily generate complex branch points via quantum loops, thus they can never appear alone and they distort usual form of dispersion relation [44], making a correct calculations more complex and more difficult. Besides the theories and models exhibiting confinement clearly, the spectrum of quarks does not need to show up confinement in some effective models. For instance quark-meson model studied in [45] provides a typical on-shell delta function in the spectral function of the quark propagator and such model does not explain confinement at all.

To get the analytical continuation in our presented study, we convert the DSEs system (written in momentum space) into a new system of equations for spectral functions as the first step. Our main goal is developing numeric, which makes the original method developed by the author earlier in [10, 12, 14, 24] actually working and useful in practice for strongly coupled theories with confinement. Actually, this second step was lacking for decades and this completion is the main purpose of presented study.

The paper's organization is as follows. In the next Section II we explain how to get spectral function within the simple model: the quenched QED in 3+1 dimensions. In the Section III we revise numeric used in [24] and offer a more precise solution for the gluon DSE there. We also make a short remark on the existing spectral solutions for the quark propagator in the Section IV.

II. STRONG QUENCHED QED IN 3+1 DIMENSIONS

Weakly coupled quenched QED in 3 + 1 dimension is certainly a theory without confinement. It contains free moving electrons in its spectrum and for α satisfying inequality $\alpha < \alpha_c$ one gets non-confining spectral solution for the fermion propagator [10]. The spectral function has a delta function associated with free propagation and continuum part above. We argue, that such solution does not exist for super-critical couplings (i.e. for the value of the coupling such that $\alpha > \alpha_c = \pi/3$), for which case we provide another -confining- spectral solution for the first time. We avoid the use of hard cutoff, introduce the electron mass term explicitly. There would be cut off dependent interplay between two effects chiral symmetry breaking and confinement. Remind the reader the mass function obey Miransky scaling $M(0) \simeq \Lambda \exp(\alpha - \pi/3)^{-1/2}$, which persists in more sophisticated approximations [46]. Therefore, since our fermion is explicitly massive in presented study, we can use several equivalent computational schemes, including dimensional regularization/renormalization [47], BPHZ scheme [48] as well as an L-operation scheme [49], all incorporate mass renormalization as usually.

Conventional renormalization schemes (dimensional or BPHZ) together with simultaneous use of the following spectral representation:

$$S(k) = \int_0^\infty da \frac{\not{k}\rho_v(a) + \rho_s(a)}{p^2 - a + i\epsilon} \quad (2.1)$$

for the fermion propagator S calls for the renormalization of the mass. The reason is that the Euclidean space loop integral turns to be divergent after changing ordering of integrations.

Our convention for Minkowski metric tensor reads: $g_{\mu\nu} = \text{diag}(+1, -1, -1, -1)$. Minkowski momenta are not labeled in our notation and we write index E when we want to specify the Euclidean momentum (i.e. $q_E^2 = -q^2$ for the square).

We restrict here to quenched ladder-rainbow approximation of the fermion DSE, which in the Landau gauge reads:

$$\begin{aligned} S^{-1} &= \not{p} - m_o - \Sigma(p) \\ \Sigma(p) &= ie^2 \int \frac{d^4k}{(2\pi)^4} \gamma^\mu S(k) \gamma^\nu \frac{P_{\mu\nu}(k-p)}{(k-p)^2 + i\epsilon}, \end{aligned} \quad (2.2)$$

where e is the fermion charge, $P(z)$ is transverse projector. Two functions or distributions $\rho_{v,s}$ in the Eq. (2.1) are enough to complete two scalar propagator functions $S_{v,s}$ (or A, B alternatively). In our notation they are defined as

$$S(p) = S_v(p) \not{p} + S_s(p) = \frac{1}{\not{p}A(p^2) - B(p^2)}. \quad (2.3)$$

DSE in dimensional renormalization scheme

Substituting the representation (2.1) into the DSE, swapping the order of integrations and making the integration over the momentum one gets

$$\begin{aligned} B(p^2) &= m_0 + \frac{3e^2}{(4\pi)^2} \int_0^\infty da \rho_s(a) \int_0^1 dt \left(\ln \left[\frac{p^2 t - a + i\epsilon}{\mu_t^2} \right] + C \right) \\ &= m(\mu_t) + \frac{3e^2}{(4\pi)^2} \int_0^\infty da \rho_s(a) \int_0^1 dt \ln \left[\frac{p^2 t - a + i\epsilon}{\mu_t^2} \right], \\ A &= 1, \end{aligned} \quad (2.4)$$

where μ_t is t'Hooft renormalization scale of MS bare dimensional renormalization scheme, which has been used.

In the next step we will add the zero of the following form

$$0 = B(\zeta) - m(\mu_t) - \frac{3e^2}{(4\pi)^2} \int_0^\infty da \rho_s(a) \int_0^1 dt \ln \left[\frac{\zeta t - a + i\epsilon}{\mu_t} \right] \quad (2.5)$$

to the rhs. of (2.4), i.e. we subtract the equation with itself evaluated at the scale ζ . We thus get

$$B(p^2) = B(\zeta) + \frac{3e^2}{(4\pi)^2} \int_0^\infty da \rho_s(a) \int_0^1 dt \ln \left[\frac{p^2 t - a + i\epsilon}{\zeta t - a + i\epsilon} \right]. \quad (2.6)$$

Note also, the function $M = B/A$ is renormalization scheme invariant here as well as in other gauges.

DSE in L- renormalization scheme

In dimensional regularization prescription and the singular pole term $1/\epsilon_d = 1/(d-4)$ in the constant C is absorbed into the renormalized mass, such that

$$m(\mu_t) = m_0 - \frac{3e^2}{(4\pi)^2} \int_0^1 da \rho_s(a) [1/\epsilon_d + \gamma_E + 4\pi] \quad (2.7)$$

Similarly, using the auxiliary Feynman integration one can get the renormalized DSE equation in the so called L -operation scheme [49]. The equation is then exactly identical to the second line in (2.4) with μ_t^2 replaced by newly introduced scale μ_F^2 and the renormalized mass reads

$$m(\mu_F) = m_0 + \frac{3e^2}{(4\pi)^2} \int_0^1 da \rho_s(a) [\ln \epsilon_z - \ln(\frac{\lambda^2}{\mu_F^2})] \quad (2.8)$$

in this scheme. Note that the scales λ as well as μ_F are arbitrary and the limit $\epsilon_z \rightarrow 0$ is understand. In this scheme the logarithmic divergence presented in the original momentum space integral turns to logarithmic divergent term but now in the Feynman parametric integral.

In order to maintain renormalizability in any known scheme, the mass term is inevitably presented, otherwise spectral representation could not be used. No matter what the amount of dynamically generated mass is, the meaning of dynamical mass generation is always limited in strong coupling QED. A pre-defined ordering of limits, which appear in theory, offers a naive definition of the chiral limit in case of vanishing integral

$$\int da \rho_s(a) = 0. \quad (2.9)$$

Since the quenched QED in 3+1D is not an asymptotically free theory, it splits to different effective models according to what regularization method is used. Massive theory used and renormalized herein can be hardly compared to cutoff theory considered for instance in [50]. Nevertheless, this is simplicity of quenched QED and appearance of confinement through the absence of free propagating modes of Lagrangian fermion field, which deserves our attention.

The method of solution

For the spacelike value of p^2 variable and for the negative ζ we can drop out Feynman $i\epsilon$ and solve the equation in the spacelike domain of Minkowski space. Note plainly, that for this purpose one should know the spectral function ρ in advance. Therefore, in order to determine the function ρ it is helpful to consider the Eq. (2.4) at the timelike scale, where the running mass B is a complex valued function. The analytical continuation of the DSE (2.6) for $p^2 > 0$ can be written as

$$\begin{aligned} \Re B(p^2) &= \Re B(\zeta) + \frac{3e^2}{(4\pi)^2} \int_0^\infty da \rho_s(a) \int_0^1 dt \ln \left| \frac{p^2 t - a}{\zeta t - a} \right|, \\ \Im B(p^2) &= -\frac{3e^2}{16\pi} \int_0^\infty da \rho_s(a) \left[\left(1 - \frac{a}{p^2}\right) \theta(p^2 - a) - \left(1 - \frac{a}{\zeta}\right) \theta(\zeta - a) \right], \end{aligned} \quad (2.10)$$

where $\theta(x)$ is the usual Heaviside step function, which reads $\theta(x) = 1$ for $x > 0$ and $\theta(x)$ is zero otherwise.

Keeping the equation for the dynamical mass function B in hand, one can reconstruct the propagator S . Comparing the real and the imaginary parts of the Eq. (2.6) and the Eq.(2.1) one can write the following complementary equation:

$$\rho_s(s) = \frac{-1}{\pi} \frac{\Im B(s) R_D(s) + \Re B(s) I_D(s)}{R_D^2(s) + I_D^2(s)} \quad (2.11)$$

where $s = p^2 > 0$ in our metric convention, and where the functions R_D and I_D stand for the square of the real and the imaginary part of the function $sA^2(s) - B^2(s)$, i.e.

$$\begin{aligned} R_D(s) &= s[\Re A(s)]^2 - s[\Im A(s)]^2 - [\Re B(s)]^2 + [\Im B(s)]^2, \\ I_D(s) &= 2s\Re A(s)\Im A(s) + 2\Re B(s)\Im B(s), \end{aligned} \quad (2.12)$$

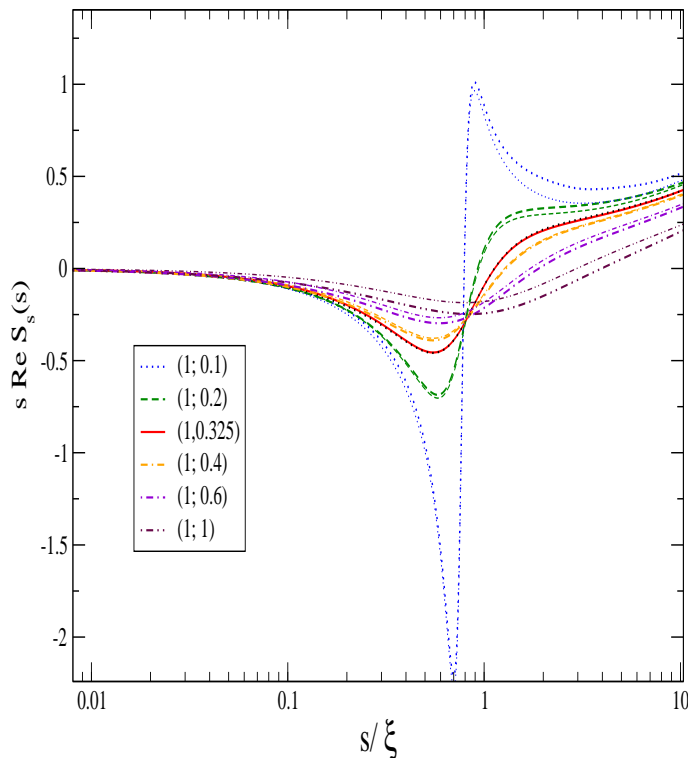


FIG. 1: $sS(s)$ function constructed from L and R functions. Each type of line corresponds to a particular choice of the phase, they are labeled by pair of numbers: real and imaginary part of $B(\zeta)/\zeta$. The exception in labeling is the true DSE solution, i.e. best matching case, where “L” is dotted, while “R” solution is depicted by the solid line.

where we keep A non constant for general purpose (note, that the Eq. $A = 1$ is valid in the approximation employed here).

To get the solution, we start with some initial guess for the constant $\Im B(\zeta)$ as well as for the trial spectral function $\rho_s(s)$ and substitute it into the Eq. (2.10). Then three equations (2.10) and (2.11) have been solved numerically by the method of iterations.

In this way, after relaxing the iteration process, irrespective of the numerical accuracy the obtained function ρ_s is still not what we are looking for. The system is ill constrained by our initial guess for the complex phase $\phi = \tan^{-1} \Im B(\zeta) / \Re B(\zeta)$. Obviously the system of equations has a rich structure of solutions among them we need to find the correct one. To get rid of the problem we fix $\Re B(\zeta)$ and repeat iteration procedure described above for a new value $\Im B(\zeta)$ and look at the quality of equality:

$$L(s) = R(s) = \frac{1}{4} \Re Tr S(s) = \Re S_s(s) \quad (2.13)$$

where

$$\begin{aligned} L(s) &= P. \int_0^\infty da \frac{\rho_s(a)}{p^2 - a} \\ R(s) &= \frac{-\Im B(s) I_D(s) + \Re B(s) R_D(s)}{R_D^2(s) + I_D^2(s)} \end{aligned} \quad (2.14)$$

for a given choice of the phase $\phi(\zeta)$. By minimizing the difference $L - R$ we identify a correct value of the phase $\phi(\zeta)$ (for which the Eq. $L - R = 0$ is hold). Note, this very similar two steps method has been successfully applied to gain a solution of DSE of the quark propagator very recently [18, 20].

Similar could be done for the function S_v (see Appendix), however in our approximation the function S_v is completely determined by the function S_s and to check the validity of Eq. (2.13) is enough. We show the results in the Fig. 1, where the solid line represents result for the propagator corresponding to the ratio $\Im B(0.1) / \Re B(0.1) = 0.325 \pm 0.005$. The real part of $B(\zeta)$ is our choice, while the imaginary part $\Im B(\zeta = 1)$ was the subject of the numerical scan. In order to visualize our numerical search, we plot two lines corresponding to L and R as defined in by (2.14). More

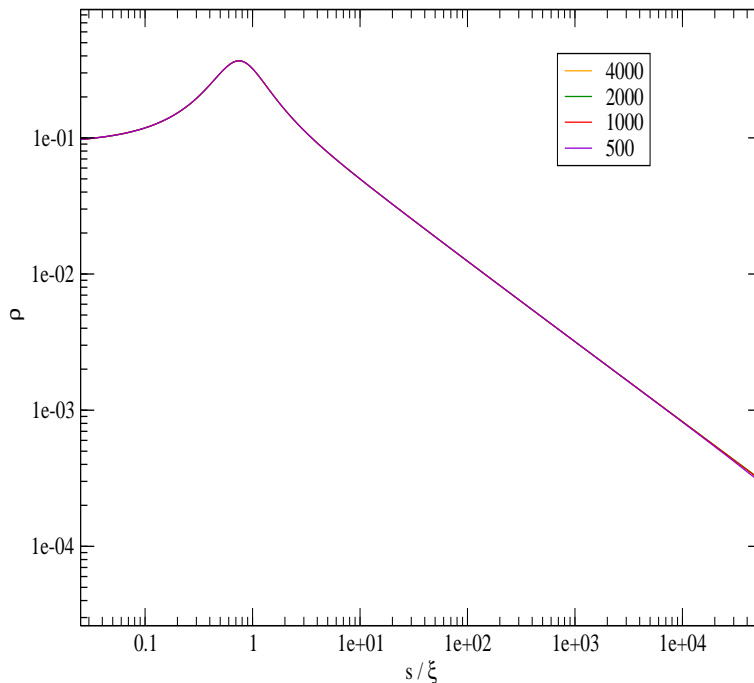


FIG. 2: Spectral function of strongly interacting fermion in units of renormalized mass ζ . Exhibition of numerical stability is manifest, note that the labeling of the lines corresponds to the number of integration points, no associated cutoff regulator dependence is observed.

L-line can be distinguished R-one, larger deviation from the equality (2.13) is observed. Lines are labeled by two numbers representing values $\Re B(\zeta)$, $\Im B(\zeta)$.

The absence of the real pole in the propagator is obvious and instead of the physical threshold the propagator has the zero branch point. Confinement is because of an abrupt generation of absorptive part of the mass function in the infrared domain of the timelike momentum. Propagator shape does not correspond to the decay of particle mode, but is associated with the creation-reabsorption process of confined modes of the fermion quantum field. It is worthwhile to mention that the generation of zero anomalous threshold is the old conjecture of Schwinger [51] made for 1+1 QED. His idea has emerged before we have accepted QCD as a correct theory of hadrons.

In non-confining quantum field theory, the Osterwalder-Schrader axiom of reflection positivity [52] is equivalent to the positive definiteness of the norm in Hilbert space of the corresponding Quantum Field Theory. Violation of reflection positivity is often regarded as a manifestation of confinement [41]. In the Fig. 2 we show the spectral function of the fermion propagator. Obviously the property of reflection positivity is not lost in our case, however the fermion turns to be a short living excitation according to suggestion made (albeit for the photon) by J. Schwinger half century ago. Violation of reflection positivity turns out to be a weak criterion for confinement in the model presented here.

We do not show the evolution of propagator functions with the coupling. Within decreasing coupling the shape of scalars $S_{v,s}$ gradually rise elbows and the on shell pole emerges for subcritical value of couplings. Thus for small couplings then one needs also to determine the pole position and its residuum as done for theory in even dimensions [10],[14] as well as in theories with odd number of spacetime dimensions [53]. We also do not go beyond quenched approximation because of the Abelian character of the interaction, but study of unquenching effects is in principle possible.

As we have already mentioned, we do not get any truly conformal solution. Perhaps, it could be doable if the superconvergent relation $\int \rho(a) = 0$ is fulfilled. This condition has never been satisfied and the solution likely does not exist at all.

III. CONFINEMENT OF GLUONS IN PURE YANG-MILLS THEORY

In this section we provide several solutions of SDE for gluon propagator as obtained by analytical continuation within integral representation method. For our purpose we will use a simple truncation introduced in [54], which was

further studied and extended in [55–57] in the Euclidean space as well as the first, not yet perfectly convergent solution in Minkowski space was attempted in [24]. To remind briefly, our calculation framework is based on nonperturbative generalization of the Background Field method [58] and used in Landau gauge for purpose of comparison with lattice data. The goal achieved here is to offer precise solution in the timelike momentum domain, which is based on the method of subtractions at the timelike scale in an exact manner described in the previous section.

For completeness we list all necessary ingredients of the gluon SDE truncation. The Schwinger mechanism is employed through the simple Ansatz for the unproper three gluon PT-BFM dressed vertex, which reads

$$d(k)\tilde{\Gamma}_{\nu\alpha\beta}(k, q)d(k+q) = \int d\omega\rho(\omega)\frac{1}{k^2-\omega+i\epsilon}\Gamma_{\nu\alpha\beta}^L\frac{1}{(k+q)^2-\omega+i\epsilon} + d(k)\tilde{\Gamma}_{\nu\alpha\beta}^T d(k+q), \quad (3.1)$$

where $\Gamma_{\nu\alpha\beta}^L$ satisfies tree level WTI and d is scalar function related to the all order PT-BFM gluon propagator which in Landau gauge reads

$$G^{\mu\nu} = \left[-g^{\mu\nu} + \frac{k^\mu k^\nu}{k^2} \right] d(k^2) \quad (3.2)$$

and satisfies usual Lehman representation

$$d(k^2) = \int_0^\infty d\omega \frac{\rho(\omega)}{k^2 - \omega + i\epsilon} \quad (3.3)$$

and $\tilde{\Gamma}_T$ is the rest of the three gluon unproper vertex which is not specified by gauge invariance. In the expression (3.3) we assume the branch point is located in the beginning of complex plane. Albeit not generated by poles, it is in its usual “non-anomalous” position.

The essential feature of the vertex $\Gamma_{\nu\alpha\beta}$ is that apart from the structure dictated by WTI it also includes $1/q^2$ pole term which gives rise to infrared finite solution. For this purpose the following form

$$\begin{aligned} d(k)\tilde{\Gamma}_T^{\nu\alpha\beta}(k, q)d(k+q) &= \int d\omega\rho(\omega)\frac{1}{k^2-\omega+i\epsilon}\Gamma_{\nu\alpha\beta}^T\frac{1}{(k+q)^2-\omega+i\epsilon} \\ \Gamma_T^{\nu\alpha\beta}(k, q) &= c_1[(2k+q)_\nu + \frac{q_\nu}{q^2}(-2k\cdot q - q^2)]g_{\alpha\beta} + [c_3 + \frac{c_2}{2q^2}((k+q)^2 + k^2)](q_\beta g_{\nu\alpha} - q_\alpha g_{\nu\beta}), \end{aligned} \quad (3.4)$$

has been proposed in [55]. This vertex is transverse with respect to q ($q\cdot\Gamma = 0$) and it respects Bose symmetry to two quantum legs interchange.

After the renormalization, it leads to the following form of SDE in Euclidean space:

$$\begin{aligned} d_E^{-1}(q_E^2) &= q_E^2 \left\{ K + bg^2 \int_0^{q_E^2/4} dz \sqrt{1 - \frac{4z}{q_E^2}} d_E(z) \right\} \\ &+ \gamma bg^2 \int_0^{q_E^2/4} dz z \sqrt{1 - \frac{4z}{q_E^2}} d_E(z) + d_E^{-1}(0), \end{aligned} \quad (3.5)$$

where the second line appears due to the Ansatz for the gluon vertex (3.4) and K is the renormalization constant. Thus, the strength of the dynamical mass generation is triggered through the adopted coupling constants c_1, c_2, c_3 , which is fully equivalent to introducing (in principle arbitrary) constant γ and infrared value $d_E^{-1}(0)$.

Analytical continuation $q_E^2 = -q^2 = -s \rightarrow q^2, s = q^2 > 0$ of the Eq. (3.5) is very straightforward and the gap equation for the gluon propagator for timelike variable s reads

$$d^{-1}(s) = s \left\{ K + bg^2 \int_0^{s/4} dz \sqrt{1 - \frac{4z}{s}} d(z) \right\} + \gamma bg^2 \int_0^{s/4} dz z \sqrt{1 - \frac{4z}{s}} d(z) + d^{-1}(0) + i\epsilon, \quad (3.6)$$

where we use standard convention $d_E(q_E^2) = -d(s)$ for $s = q^2 < 0$ and absorb the sign into the definition of Minkowski space gluon propagator. Note, the inverse propagator $d^{-1}(0)$ should take a negative value to prevent tachyonic solution.

Subtracting the equation once again at the timelike fixed scale ζ one gets:

$$\begin{aligned} d^{-1}(s) &= s \left\{ K + bg^2 \int_0^{s/4} dz \sqrt{1 - \frac{4z}{s}} d(z) \right\} - (s \rightarrow \zeta) \\ &+ \gamma bg^2 \int_0^{s/4} dz z \sqrt{1 - \frac{4z}{s}} d(z) - (s \rightarrow \zeta) - d^{-1}(\zeta). \end{aligned} \quad (3.7)$$

Now, the function d is assumed to be complex for all $s > 0$, while it stays real for negative s .

Like in previous study of strong coupling QED, the phase of the propagator needs to be tuned to get desired analytical property. The numerical search of the phase of the function $d(\zeta)$ is performed such that we fix the real part $\Re d^{-1}(\zeta)$ and then look for the value of $\Im d^{-1}(\zeta)$ till assumed integral representation, e.g. the following relation

$$\Re d(k^2) = \frac{-1}{\pi} P. \int d\omega \frac{\Im d(\omega)}{k^2 - \omega}, \quad (3.8)$$

holds for all momenta.

Detailed values of renormalization constant K and d^{-1} are not crucial for the subject of confinement, however they need to be tuned to get agreement with the lattice data. As a first we present the solution of SDE governed by the Gauge Technique and take the transverse term very small for this purpose, numerically we put $\gamma = 1/20$ in the second term in (3.7). Further we set the coupling $g^2 = 15.5$ and for renormalized propagator the condition $\Re \zeta d(\zeta) = 1.8570$ and $K(\zeta) = 1$ was chosen. Searching for correct analyticity we obtained $\Im \zeta d(\zeta) = 0.140$ at fixed $\zeta = 1 GeV$ after the iterations. This Gauge technique governed solution is shown in the Fig. 4 for the timelike momenta. Note the smooth solution for the spacelike momenta is not shown, and we just note it is several times smaller the lattice data in the infrared domain, hence non-compatible at all.

The solution, which complies reasonably with the lattice data [59–61] is shown in figures 3 and 5 where in the later case the comparison with lattice fit is made. A relatively large coupling for transverse component of the vertex was needed to make the solution comparable to lattice gluon propagator in the infrared. The excellent small error difference $\sigma^2 = 3.510^{-5}$ was achieved for difference between lhs and rhs of equation (3.8), showing that desired analytical properties can be achieved with high accuracy. Obviously the SDE solution and the lattice data doesn't agree completely as our transverse component was modeled and not a complete vertex. Better agreement between the lattice and the SDE solution would require approximation improvement, e.g. by inclusion of not yet considered transverse component of triple vertex component. Perhaps the inclusion of ghost loop should improve numerical agreement as well.

Numerically, our solution was obtained within the following couplings: $\gamma = -4.5$ and $g^2 = 2.167$, and the renormalization and complex phase was determined by values $\Re d(\zeta) = 8.323 * 10^{-2} GeV^2$; $\Im \zeta d(\zeta) = 7.5810^{-3} GeV^2$ at the timelike renormalization scale $\zeta = 2.89 GeV$. In this case we found advantageous to reduce the constant, such that $\Re K = 1/2$ was taken and $\Im K = 7.3 * 10^{-2}$ was iteratively searched value. Codes running at the end of iteration cycles are available at author's web page (questions can be asked via email).

At ultraviolet the studied gluon propagator vanishes as $1/s \ln^\kappa(s)$ with $\kappa \simeq 0.5$ (the size of κ is understand mainly because of Landau gauge used in primitive truncation here). This behavior should lead to super-convergent relation sum rule [62],[63],[64]:

$$I = \int_0^\infty \rho(s) ds = 0, \quad (3.9)$$

which turns to be satisfied with reasonable accuracy $I \simeq 0.05$

In both presented numerical solutions: the Gauge Technique like and lattice like one, the shape of the gluon propagator at the timelike region is obviously something what we are not experienced (see the Fig. 4 and the Fig. 3 respectively). The real part of the function d is represented by two broad peaks with mutually opposite signs. However let us recall here, that kind of the resonance with zero mass anomalous threshold of the form

$$\rho(s) = \frac{Cs}{(s^2 - s_o^2)^2 + (s\Gamma)^2} \quad (3.10)$$

was suggested as an artificial mathematical model for the spectral function of the photon in the Schwinger model [51]. Interestingly, the spectral gluon function can be accurately estimated as a difference of two such excitations. Because of the asymptotic freedom, instead of using (3.10), more suited fit can be constructed from the sum of modified Cauchy distributions, instead of using (3.10) and we take

$$\rho(s) = \Sigma_i [R \frac{(s/\zeta)^\lambda}{(s - s_o)^2 + (\Gamma)^2}]_i, \quad (3.11)$$

where the exponent $\lambda = 0$ for the positive modes of the function ρ (negative modes in figures), while for the negative mode the exponent $\lambda = 3/4$ was taken. Only two such contribution are enough to describe the gluon propagator in the infrared domain of momenta. Fitting the first peak structure at 800MeV, the second peak then appears at 1110 MeV for Gauge Technique governed solution.

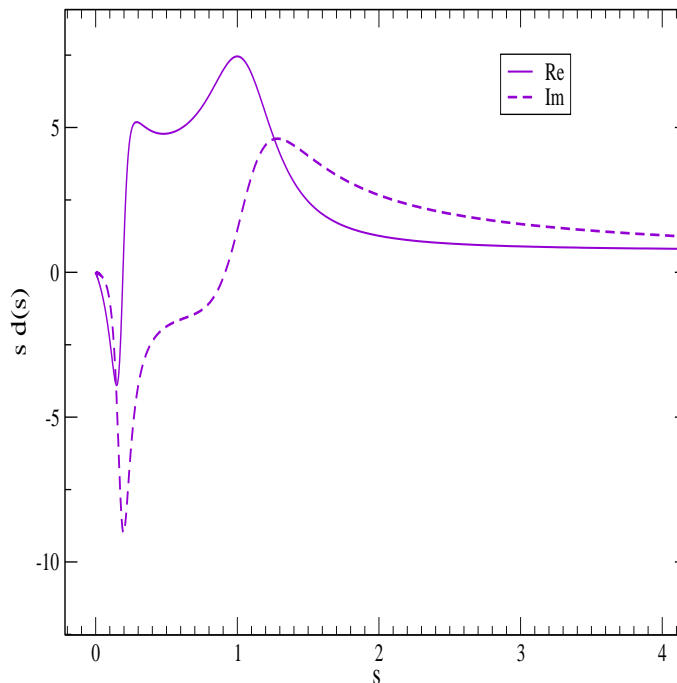


FIG. 3: Lattice like solution of SDE for the gluon propagator plotted at the timelike domain of momenta against $s = p^2$ in units of GeV^2 . The first peak is located at $445MeV$.

More interestingly, performing similar fit for the lattice like solution, one gets the position of the first peak $\mu_g = 450MeV$, while much broad peak of opposite sign is located nearly at $1GeV$ (see again the Fig. 4). For the gluon mass scales estimated by others, see for instance [11] $\mu_g = 500 \pm 200MeV$ and [68] $\mu_g \simeq 0.5GeV$.

Let us stress here that the gluon propagator is intrinsically unphysical quantity and neither of fit presented here follows any experimental data. All presented scales (which is the only number we need for a given fit) could be understand as educated estimate coming from gauge invariant considerations -string tension, meson masses or decay constants- performed in the Landau gauge.

Actually, among other choices, it is the Landau gauge that was extremely popular and preferred in SDEs studies during last decades. However, as very well known (see for instance [67]) changes within varied gauge fixing parameter are shown to be dramatic in the sector of unphysical gluon and ghost propagators. Hence to understand confinement in QCD properly, one could be able to build gauge (fixing) invariant quantity in framework of SDEs and to the best provide the hadronic form factor for arbitrary gauge. To this point a departure from popular Landau gauge turns to be an advantageous choice. We briefly mention a limited progress made in this direction in the following section.

IV. SHORT REMARK ON THE QUARK PROPAGATOR

Following similar method described in the Sect. 2, the ladder-rainbow approximation (LRA) for the quark SDE has been already solved in the paper [20] in other gauges than Landau gauge. The obtained quark propagator has an anomalous threshold located at or very near beginning of complex plane of square of momenta and the confinement of quarks manifests as missing real pole in the quark propagator. Interested reader can find the details in the paper [20].

As an interesting task we have accomplished the same approximation as in the paper [20], but with kernel given by the Landau gauge gluon propagator instead. As a matter of fact, such approximation neither provides a known slope of the quark dynamical mass function or correct pion observable (mass and decay constant f_π). Hence neither such approximation can be used to calculate continuous form factor. A possible understanding of this inefficiency is obvious from the modern version of Goldberger-Treiman-like relation [65],[66], which reads

$$f_\pi \Gamma_A(0, k) = B(k) \quad (4.1)$$

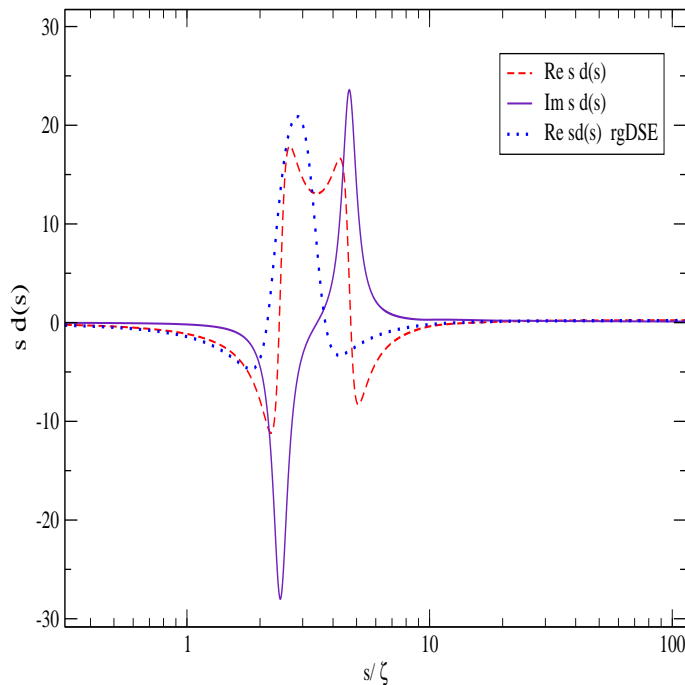


FIG. 4: Gauge Technique governed SDE solution for gluon propagator plotted at the timelike domain of momenta (in units of renormalization scale ζ). The real part of the solution for the so called Renormgroup improved SDE (see [24] for the meaning) is added for comparison.

where Γ_A is the leading piece of the pion's Bethe-Salpeter amplitude and B is the quark dynamical mass times the quark renormalization function. As can be seen from the quark DSE only trivial solution for the rhs. of E. (4.1) exists. In other words, a single gluon exchange approximation with Landau gauge gluon propagator underestimates of the true strength of the quark-antiquark interaction.

Miraculously, the picture is dramatically changed when one leave the Landau gauge and utilize exactly the same method but for larger gauge fixing parameter. The pions are then true Goldstone bosons correctly generated in such model within LRA, where the gluon propagator is strengthened by presence of large longitudinal modes in the quark-antiquark interacting kernel. Actually a few existing calculations provide first hints for working scheme of SDEs solutions within a sort of integral representations for QCD/QED Green's functions. Of course, the calculation of continuous form factors are not easy in presented scheme and various approximations limit the method in practice at these days. The reader can find the first applications in calculation of meson transition and the meson electromagnetic form factor in [18, 21, 22]

V. CONCLUSION

We have applied the method of subtractions to SDEs at the timelike scale of momenta and get the confined solution in Yang-Mills theory for the gluon propagator as well as for the fermion propagator in quenched QED. In both strong coupling models, the solutions for two point correlator were obtained in the entire domain of Minkowski space momenta. When used in other gauges or in more sophisticated approximations, the method is a possible candidate for numerical evaluation of hadronic form factors needed to describe a production processes in hadronic physics. We do not incorporate complex conjugated poles, which are nowadays seen numerically in spectra of lattice propagators of confined fields [39]. They were not necessary for solutions presented here. On the other side, if complex conjugated poles are not a gauge dependent and numerical artifact and they will become a rigid analytical structure of QCD correlator, they need to be incorporated properly. While, this is certainly possible by deforming the integration contours, the presence of them requires access to entire complex plane and would make the evaluation extremely demanding. For a nice discussion of this open problem, see recent paper [44], where consequences of embedding the complex conjugated poles into the gluon propagator are shown for a simple truncation of ghost/gluon DSEs system in a pure Yang-Mills sector. Obviously, a search of calculation scheme with limited amount of non-holomorphic singularities is worthwhile to search in QCD and other strong coupling quantum field models with confinement as

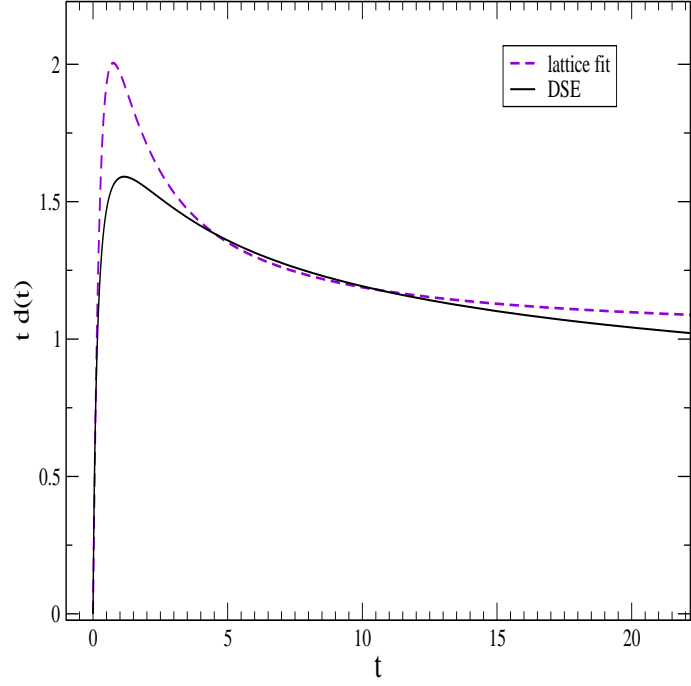


FIG. 5: Lattice like solution of gluonic SDE compared to the conventional lattice fit [59, 60] in the Landau gauge.

well.

Appendix A: Appendix A

The second constrains which should be checked beyond ladder-rainbow approximation can be derived by making the trace of \not{p} -projected fermion propagator, where

$$L_v(s) = R_v(s) = \frac{1}{4p^2} \Re \not{p} Tr S(s) = \Re S_v(s). \quad (\text{A1})$$

with the left and right hand sides defined as

$$\begin{aligned} L_v(s) &= P. \int_0^\infty da \frac{\rho_v(a)}{s-a} \\ R_v(s) &= \frac{-\Re A(s) R_D(s) + \Im A(s) I_D(s)}{R_D^2(s) + I_D^2(s)} \end{aligned} \quad (\text{A2})$$

where symbol $P.$ stands for principal value integration.

-
- [1] T. Appelquist, D. Nash, and L.C.R. Wijewardhana, Phys. Rev. Lett. **60**, 2575 (1988).
 - [2] A. Kocis, Phys. Lett. B **189**, 449 (1987).
 - [3] C. J. Burden, J. Praschifka and C. D. Roberts, Phys. Rev. D **46**, 2695 (1992).
 - [4] C.S. Fischer, R. Alkofer, T. Dahm and P. maris, Phys. Rev. D **70**, 073007 (2004).
 - [5] P. Maris, Phys. Rev. D **52**, 6087 (1995).
 - [6] N. Dorey and M.A. mavromatos, Nucl. Phys. B **386**, 614 (1992).
 - [7] M. Franz and Z. Tesanovic, Phys. Rev. Lett. **87**, 257003, (2001).
 - [8] I. F. Herbut, Phys. Rev. Lett. **94**, 237001 (2005).
 - [9] V.P. Gusynin, S. G. Sharapov and J.P. Carbotte, Int. J. Mod. Phys. B **21**, 4611 (2007).
 - [10] V. Sauli, JHEP **7** (2), 1-36, (2003).
 - [11] J.M. Cornwall, Phys. Rev. D **26**, 1453 (1982).

- [12] V. Sauli, J. Adam, Phys. Rev. D **67**, 085007 (2003).
- [13] R. Delbourgo and P.C. West, J. Phys. A **10**, 1049 (1977).
- [14] V. Sauli, Few Body Syst. **39**, 45 (2006).
- [15] C. N. Parker, J. Phys. A, Math. Gen. **17**, 2873 (1984).
- [16] V. Sauli, J. Adam, P. Bicudo, Phys. Rev. D **75**, 087701 (2007).
- [17] C. Mezraga and G. Salme, Eur. Phys. J. C **81** 1,34 (2021).
- [18] V. Sauli, Phys. Rev. D **102**, 014049 (2020).
- [19] C. Mezrag, G. Salme, Eur. Phys. J. C **81**,1 (2021).
- [20] V. Sauli, Few Body Syst. **61**, 3, 23 (2020).
- [21] E. Ydrefors, W. Paula, J.H.A. Nogueira, T. Frederico, G. Salme, arXiv:2106.10018.
- [22] V. Sauli, arXiv:2204.08424.
- [23] D. C. Duarte, T. Frederico, W. Paula, E. Ydrefors, arXiv:2204.08091.
- [24] V. Sauli, J. Phys. G **39**, 035003 (2012).
- [25] V. Gribov, Nucl. Phys. B **139**, 1 (1978).
- [26] D. Zwanziger, Nucl. Phys. B **321**, 591 (1989).
- [27] D. Epple, H. Reinhardt, W. Schleifenbaum, Phys. Rev. D **75**, 045011 (2007).
- [28] G. 't Hooft, Nucl. Phys. B **138**, 1 (1978).
- [29] P. Vinciarelli, Phys. Lett. B **78**, 485 (1978).
- [30] T. Yoneya, Nucl. Phys. B **144**, 195 (1978).
- [31] J.M. Cornwall, Nucl. Phys. B **157**, 392 (1979).
- [32] G. Mack, V.B. Petkova, Ann. Phys. **123**, 442 (1979).
- [33] H.B. Nielsen, P. Olesen, Nucl. Phys. B **160**, 380 (1979).
- [34] L. Del Debbio, M. Faber, J. Greensite, S. Olejnik, Phys. Rev. D **55**, 2298 (1997).
- [35] K. Langfeld, H. Reinhardt, O. Tennert, Phys. Lett. B **419**, 317 (1998).
- [36] L. Del Debbio, M. Faber, J. Giedt, J. Greensite, S. Olejnik, Phys. Rev. D **58**, 094501 (1998).
- [37] J. D. Stack, W. W. Tucker, Roy J. Wensley, Nucl. Phys. B **639**, 203 (2002).
- [38] Z. Zhu, K. Raya, L. Chang, Phys. Rev. D **103**, 034005 (2021).
- [39] D. Binosi, R.A. Tripolt, Phys. Lett. B **801**, (2020) 135171 (2020).
- [40] C.D. Roberts and A. G. Williams, Prog. Part. Nucl. Phys. **33**, 477-575 (1994).
- [41] R. Alkofer and L. von Smekal, Phys. Rept. **353**, 281 (2001).
- [42] D. Dudal, O. Oliveira, and P. J. Silva, Phys. Rev. D **89** 1, 014010 (2014).
- [43] R.-A. Tripolt, P. Gubler, M. Ulybyshev, L. Von Smekal, Comput. Phys. Commun. **237**, 129–142 (2019).
- [44] J. Horak, J.M. Pawlowski, N. Wink; On the complex structure of Yang-Mills theory; arXiv:2202.09333.
- [45] R.A. Tripolt, J. Weyrich, L. Smekal, J. Wambach Phys. Rev. D **98**, 094002 (2018).
- [46] A. Bashir, A. Raya, S. Sanchez-Madrigal, Phys. Rev. D **84**, 036013 (2011).
- [47] Gerard 't Hooft, M.J.G. Veltman, Nucl. Phys. B **44**, 189-213 (1972).
- [48] N.N. Bogoliubov and O. S. Parasyuk, Dok. Akad. Nauk SSSR **100**, 25–28 (1955).
- [49] V. Sauli, arXiv:2009.07195.
- [50] R. Fukuda, T. Kugo, Nucl. Phys. B **117**, 250 (1976).
- [51] J. Schwinger, Phys. Rev. **128**, 2425-2429 (1962).
- [52] K. Osterwalder and R. Schrader, Commun. Math. Phys **31**, 83 (1973). Commun. Math. Phys. **42**, 281 (1975).
- [53] J. Horak, J. M. Pawlowski, N. Wink arXiv: 2006.09778.
- [54] D. Binosi, J. Papavassiliou, Phys. Rept. **479**, 1-152 (2009).
- [55] A.C. Aguilar, J. Papavassiliou, JHEP 0612:012, (2006).
- [56] J. M. Cornwall, Phys. Rev. D **80**, 096001 (2009).
- [57] A. C. Aguilar, D. Binosi, J. Papavassiliou, Phys. Rev. D **84**, 085026 (2011).
- [58] A. Pilaftsis Nucl. Phys. B **487**, 467-491 (1997).
- [59] D. Dudal, O. Oliveira, P. J. Silva, LATTICE2018 (2018) 321; arXiv:1811.11678.
- [60] D. Dudal, O. Oliveira, M. Roelfs, P. Silva, Nucl. Phys. B **952**, 114912 (2020).
- [61] A. G. Duarte, O. Oliveira, P. J. Silva, Phys. Rev. D **94**, 014502 (2016).
- [62] R. Oehme and W. Zimmermann, Phys. Rev. D **21**, 471 (1980).
- [63] R. Oehme, Phys. Lett. B **252**, 641–646 (1990).
- [64] J. M. Cornwall, Mod. Phys. Lett. A **28**, 1330035 (2013).
- [65] P. Maris, C. D. Roberts and P. C. Tandy, Phys. Lett. B **420**, 267 (1998).
- [66] S.-X. Qin, C. D. Roberts and S. M. Schmidt, Phys. Lett. B **733**, 202 (2014).
- [67] M. Napetschnig, R. Alkofer, M. Q. Huber, J. M. Pawlowski, Phys. Rev. D **104**, 054003 (2021).
- [68] A. C. Aguilar, M. N. Ferreira, C. T. Figueiredo, J. Papavassiliou, Phys. Rev. D **100**, 094039 (2019).